# Ortho-Fluorination of azophenols increases the mesophase stability of photoresponsive hydrogen-bonded liquid crystals

# Journal of Materials Chemistry C

## ARTICLE

# *Ortho*-fluorination of azophenols increases the mesophase stability of photoresponsive hydrogen-bonded liquid crystals†

Marco Saccone[a,b], Kim Kuntze[a], Zafar Ahmed[a], Antti Siiskonen[a], Michael Giese[b] and Arri Priimagi[*a]

Photoresponsive liquid crystals (LCs) whose alignment can be controlled with UV-Visible light are appealing for a range of photonic applications. From the perspective of exploring the interplay between the light response and the self-assembly of the molecular components, supramolecular liquid crystals are of particular interest. They allow elaborating the structure-property relationships that govern the optical performance of LC materials by subtle variation of the chemical structures of the building blocks. Herein we present a supramolecular system comprising azophenols and stilbazoles as hydrogen-bond donors and acceptors, respectively, and show that *ortho*-fluorination of the azophenol dramatically increases the thermal stability of the LC phases, an important characteristics in their further utilization in photonics. The systems exhibit fast photoinduced order-disorder transitions, and rapid recovery of the liquid-crystalline state once the light irradiation is ceased, due to the photochemical properties of azophenols.

## Introduction

Combining order and mobility in a unique way, liquid crystals (LCs) offer an interesting basis for the design of functional and stimuli-responsive materials.[1–3] The application potential of LCs is demonstrated by the flourishing flat-panel display technology in contemporary electronics.[4] At the same time, LCs constitute an ideal platform for exploring the interplay between self-assembly and stimuli-responsiveness.[3,5] Controlling the molecular alignment via external stimuli brings about possibilities for applications in, *e.g.*, tunable photonics[6–9] and light-to-mechanical-energy conversion[10] in case of liquid-crystal elastomers or polymer networks. As a remote and non-invasive stimulus, light is attractive for controlling LC molecular alignment. In this context, azobenzenes have gained particular attention: they are efficient molecular switches due to their large and reversible shape-change upon photo-isomerization between *trans*- and *cis*-states.[11] Depending on the thermal half-life of the latter, the photomodulated state can be temporally stable (i.e., maintained also after ceasing the irradiation)[12] or dynamic (the initial state is retained once the irradiation is ceased)[13].

During the latter half of the 20th century, the rise of supramolecular chemistry provided to the concurrently growing liquid crystal community a powerful tool for the assembly of supramolecular LC structures.[14] The advantages of using the supramolecular approach as compared to conventional single-molecule-based mesogens is manifold. Assembling mesogens from small molecules interacting via non-covalent forces such as hydrogen or halogen bonds is extremely versatile since it allows simple synthetic access to a plethora of complex self-assembled structures, finely tuned by subtle variation in the chemical structure of the starting components.[15,16] This, in turn, enables detailed and systematic structure–property relationship studies by analyzing libraries of supramolecular LC structures.

Among specific non-covalent interactions, hydrogen bonding is of particular interest considering its relatively large strength and importance in biological systems. Many examples of hydrogen-bonded LCs exist in the literature.[14,17] For instance, Kato and Fréchet investigated self-assembled liquid crystals based on dimerization of benzoic acid groups and pyridyl derivatives.[18–23] Later, Bruce and coworkers demonstrated that also phenols are suitable proton donors for the formation of hydrogen-bonded assemblies with liquid-crystalline properties.[24,25] Since the late 1980s, Percec and coworkers investigated the hierarchical self-assembly of hydrogen-bonded LC dendrimers and dendrons into complex suprastructures. From these studies they were able to deduce rational design principles for the prediction of the 3D architectures of building blocks with high fidelity.[15] Hydrogen bonding has also proven useful in stabilizing liquid crystalline blue phases.[26,27] Halogen bonding, on the other hand, is a much less studied interaction in the context of supramolecular LCs, yet in the past few years interesting examples of photocontrollable halogen-bonded LCs have been demonstrated.[28–30]

Shortly after the introduction of the first functional LC materials,[31] it was shown that fluorination at the core position of rigid molecules such as terphenyls gives them superior properties in terms of highly

negative dielectric anisotropy $\Delta\varepsilon$ (if laterally substituted) and very low ion-solvation capability, in comparison to other LC materials such as 4-cyano-4'-pentylbiphenyl and its analogues.[2,32,33] This is due to the high polarity of the C–F bond and the low polarizability of fluorine atoms.[34,35] Given the exceptional properties LCs provided by the introduction of organic fluorine, it is pertinent to elaborate the role of fluorination on supramolecular materials, which is the aim of the present work.

It has been recently demonstrated that halogen-bonded liquid-crystalline dimers comprising azobenzene and stilbazole units exhibit interesting photoinduced phase transition behavior, pinpointing the efficacy of the photocontrol over LC molecular order also in the context of supramolecular LCs.[30] In 2016, a modular approach to a series of photoresponsive hydrogen-bonded LC assemblies based on phloroglucinol and azopyridines has been reported, proving that the mesophase morphology and the photo-response is controlled by the architecture of the hydrogen-bond-donating unit.[36,37] The same modular methodology has been employed to investigate the impact of fluorination on the LC properties of hydrogen-bonded assemblies that were further used as molecular guests in order to tune the photonic properties of chiral-nematic mesoporous silica films.[38,39,40] In the above studies, fluorination (i) boosts the noncovalent interaction that drives the LC formation, (ii) modifies the photochemical properties of the azobenzenes, and (iii) contributes to stabilization of the mesophase. Yet further studies are needed to understand the role of fluorination in supramolecular LCs in order to use it in the design of high-performance photoresponsive supramolecular materials.

Herein, we combine the above approaches and design photoresponsive fluorinated supramolecular LCs of azobenzene-based bond donors and stilbazole acceptors, yet employ the strong phenol-pyridine hydrogen bonding as supramolecular synthon. We particularly focus on the role of *ortho*-fluorination of the azophenol moiety, and show that difluorination is in fact a prerequisite for the formation of enantiotropic LC phases. A detailed structure–property relationship study of azophenol:stilbazole assemblies was performed and complemented by computational investigations to rationalize the differences between the complexes.

## Results and Discussion

### At the molecular level: material design and spectral properties

The materials used in the present work are shown in **Fig. 1**. For the formation of the dimeric assemblies 4,4'-alkoxystilbazoles derivatives were used as hydrogen-bond-acceptors and as donating species, photo-switchable 4-(4'-alkylphenylazo)phenols were chosen. The individual building blocks did not show any liquid crystalline behavior, while the complexes connected by a single O-H···$N_{pyr}$ hydrogen bond revealed liquid crystalline properties for most of the samples. The chemistry of stilbazoles and their complexes has been pioneered by Bruce and coworkers who have reported several breakthroughs in supramolecular liquid crystals.[14,24,41] On the other hand, 4-(4'-alkylphenylazo)phenols are versatile building blocks that have proven useful in building functional polymeric self-assemblies,[42–45] but to the best of our knowledge have not been utilized in devising supramolecular small-

molecule-based liquid crystals. The non-fluorinated azophenol **A** (99% purity) was purchased from TCI Europe and used as received. The di-fluorinated (**B-n**) azophenols were prepared by diazotization and azo coupling reactions (see ESI for full synthetic details). The hydrogen-bond acceptors **St-n** were prepared according to literature methods.[41]
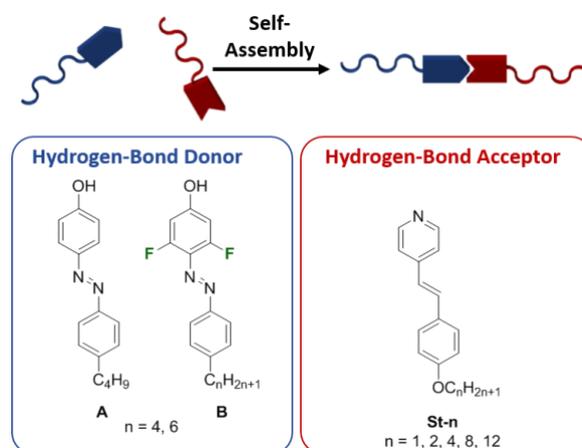


**Fig. 1** The materials concept of the present study for the investigation of the impact of fluorination in hydrogen-bonded dimers.

In our materials design, fluorination serves multiple purposes. Firstly, substitution of the azobenzene with electronegative fluorine atoms is expected to increase the strength of the O-H···$N_{pyr}$ interaction, as detailed later on. Secondly, *ortho*-fluorination of the azobenzene core is at present the most powerful strategy to increase the thermal lifetimes of the *cis*-isomers as well as to separate the n-π* transitions of the *trans* and *cis* isomers, enabling quantitative and bidirectional photoswitching.[46,47] In the context of azophenols that are known to exhibit hydrogen-bond-induced tautomerization that significantly reduces the *cis*-lifetime in polar environments,[42,48,49] fluorination has not been studied. Thirdly, it is nowadays well established that perfluorinated alkyl chains dramatically change the properties of liquid crystalline assemblies formed by dendrons,[50] block copolymers,[51] and small molecules.[52] However, such studies are almost absent for fluorinated arene species involved in supramolecular LC formation, and we are only aware of the work of Spengler *et al*. who investigated the tetrameric complexes formed by mono-fluorinated and non-fluorinated phloroglucinol and partially fluorinated azopyridine derivatives.[38] In their case, the LC phase was suppressed by azopyridine *ortho*-mono-fluorination, while addition of second fluorine resulted in formation of smectic phases and core fluorination stabilized the LC phase.[38] Therefore, we anticipate the fluorination of the photoresponsive hydrogen-bond donor not only to modify the photochemical properties and interaction strength, but also significantly affect the LC phases.

The photoisomerization of **A** and **B-n** was first studied in dilute acetonitrile and toluene solutions. **B-4** and **B-6** exhibited identical properties, thereby only the latter is considered here. The π–π* bands at 349 nm (**A**) and 339 nm (**B-n**) decreased upon irradiation

with 365 nm light, signaling efficient *trans–cis* photoisomerization and photostationary state consisting of almost solely *cis*-isomers (**Fig. 2a**). When the irradiation was ceased, the molecules relaxed thermally back to the *trans*-state, as shown in **Fig. 2b** for **B-6** in toluene. The absorption maxima and *cis*-lifetimes for **A** and **B-6** are gathered in **Table 1**. Interestingly, the *cis*-lifetimes of **B-n** were notably shorter than for **A**, in both toluene and in acetonitrile, contradicting the above-mentioned *cis*-stabilizing effect of *ortho*-fluorination reported by Bléger *et al*.[49,50] We attribute this to the increased acidity of the phenolic proton, which we believe to promote the tautomerization process and thereby increase the *cis*-to-*trans* isomerization rate. Both molecules display significantly longer *cis*-lifetime in non-polar toluene than in polar acetonitrile ($\tau_{toluene}/\tau_{ACN} > 10^3$), which is well in line with the work of Velasco *et al.* on non-fluorinated azophenols.[51-53]
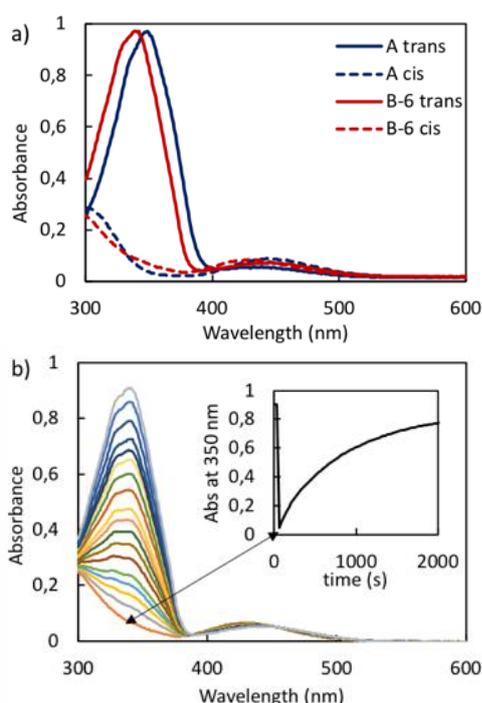


**Fig. 2** a) Normalized absorption spectra of **A** and **B-6** in relaxed (*trans*) and photostationary (*cis*) states in toluene at 25 °C, and b) thermal relaxation of **B-6** in toluene from photostationary state (inset) to *trans*, indicated by the increasing absorption at the π–π* band.

**Table 1.** Absorption maxima $\lambda_{max}$ (in toluene) and *cis*-lifetimes τ for azophenols **A** and **B-6** in acetonitrile and in toluene.

|  | $\lambda_{max}$ (nm) | $\tau_{ACN}$ (s) | $\tau_{toluene}$ (min) |
|---|---|---|---|
| **A** | 349 | 1.11 | 40.4 |
| **B-6** | 339 | 0.49 | 14.1 |

**From molecules to supramolecular dimers and liquid crystals**

The 1:1 complexes between the hydrogen-bond donors and acceptors schematized in **Fig. 1** were prepared by separately dissolving the molecules in chloroform, mixing the solutions and letting the solvent evaporate. The resulting powders were then annealed at 140 °C for 5 min to remove any residual solvent, before subjecting to further analysis.

We first studied the hydrogen-bond strengths of the dimers via density functional theory. The long alkyl chains at the *para*-positions were expected to have a negligible effect on the bond strengths and were truncated to methyl groups in order to reduce computational costs. The resulting hydrogen-bond donors are referred to as **A-1** and **B-1**. The geometries of the assemblies **A-1•St-1** and **B-1•St-1** were optimized using the PBE0/6-31+G(d,p) method. The hydrogen bond strengths were computed using the same method, and the Boys and Bernardi counterpoise correction was used to correct for the basis set superposition error.

The assembly **A-1•St-1** shows the weakest hydrogen bond (interaction energy -12.2 kcal/mol). As a reference, the interaction energy of **St-1** with an unsubstituted phenol is -10.7 kcal/mol, pointing out that the electron-withdrawing azo group increases the hydrogen bond strength. The strongly electron-withdrawing fluorine atoms in **B** increase the interaction energy to -14.1 kcal/mol. The **B-1•St-1** assembly also has a higher calculated dipole moment (11.60 D), as opposed to 10.42 D for **A-1•St-1**. Hence both the interaction strength and the dipole moment scales in the order **B > A**.

The hydrogen-bond-driven complex formation was also verified using infrared spectroscopy. The biggest changes upon complexation are observed in the OH region. This is clearly evident in the infrared spectrum of the complex **St-1•B-4** (see **Table 2**). The O–H peak of the azophenol at 3335 cm^{-1} is replaced by a broad band in the complex centered at ca. 2500 cm^{-1}. This is indicative of the formation of a strong hydrogen bond in the complex.[24] It is also known that hydrogen bonding between pyridine and phenol moieties leads to a hypsochromic shift and intensity decrease of the pyridine bands in the region 3000–3100 cm^{-1} and 1500–1590 cm^{-1}.[24] The C–H absorption of the pure stilbazole at 3021 cm^{-1} becomes less intense upon complexation and shifted to 3027 cm^{-1} as a result of a higher positive charge on the pyridyl hydrogens in the complex. A blue shift is also observed for the three bands associated with the pyridine ring breathing vibrations at 1585, 1507, and 1415 cm^{-1}. On the other hand, due to an increased electron density of the fluorinated ring upon hydrogen bonding formation, the vibrations related to the fluorophenyl moiety at 1436 cm^{-1} for the *o*-difluorophenol ring in pristine **B-4** are red-shifted to 1431 cm^{-1} upon complex formation. Finally, the pyridyl ring stretching at 981cm^{-1} is more blue shifted when complexed with the fluorinated **B-4** molecule (1011 cm^{-1}) compared to the **A** molecule (1007 cm^{-1}), which hints towards stronger hydrogen bonding between **B** and **St-1** than for the **A•St-n** complex, as expected based on computational studies.

**Table 2**. Selected infrared absorption bands (cm$^{-1}$) of the starting modules **B-4** and **St-1**, and the **B-4•St-1** complex.

|  | B-4 | St-1•B-4 | St-1 |
|---|---|---|---|
| Pyridyl *C–H* stretching |  | 3027 | 3021 |
| Pyridyl *ring breathing* |  | 1589 | 1585 |
| Pyridyl *ring breathing* |  | 1509 | 1507 |
| Pyridyl *ring breathing* |  | 1420 | 1414 |
| Phenol *O–H* stretching | 3335 | ~ 2500 |  |
| Phenol *C–F* stretching | 1436 | 1431 |  |

The LC phase behavior of the complexes was analyzed by hot-stage polarized-optical microscopy (POM) and differential-scanning calorimetry (DSC). As expected, none of the starting materials was liquid crystalline. The complexes between the non-fluorinated 4-(4'-buthylphenylazo)phenol **A** with the stilbazoles **St-n** were analyzed by POM using a scanning speed of 5 °C/min. To our surprise, exclusively the complex **A•St-12** showed a monotropic smectic A (SmA) phase (ΔT = 15 °C), while none of the other complexes exhibited liquid crystallinity (**Fig. 3**).
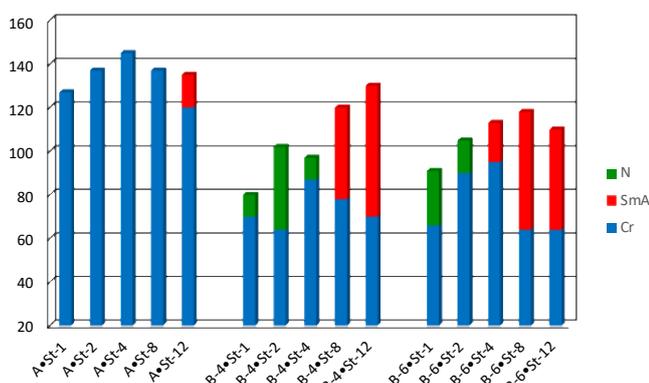


**Fig. 3**. Chart summarizing the thermal behavior of **A** and **B-n** complexes with the stilbazoles **St-n**. The transitions are reported upon cooling (5 °C/min) for **A•St-n** and upon heating (5 °C/min) for **B-n•St-n**.

The two series of complexes based on *ortho*-difluorinated azobenzene **B-n** with stilbazoles, **B-4•St-n and B-6•St-n**, exhibited very different behavior as compared to the **A•St-n** complexes. In general, when compared to the **A·St-n** assemblies, the transition temperatures from the crystalline to the isotropic/liquid-crystalline state decreased significantly, by *ca*. 50 °C on average. Enantiotropic mesomorphism with a rich variety of LC phases and broad LC temperature range (even exceeding 50 °C upon heating) was observed by POM. Representative textures of the different phases are shown in **Fig. 4**, and similar textures were observed also for the other complexes under investigation (ESI). Upon cooling, the LC phases were even broader due to supercooling, and could be maintained even close to room temperature (see the SI for further details). The **B-4**- and **B-6**-based complexes showed rather similar thermal behavior. For both systems, an increase in the transition temperatures from the mesophase to the isotropic state was found

with increasing length of the alkyl chain at the stilbazoles, with the exceptions of **B-4•St-4 and B-6•St-12**, for which slight decrease in the clearing points were observed as compared to **B-4•St-2 and B-6•St-8**, respectively. With respect to the mesophase morphology, nematic (N) phase (**Fig. 4a**) was observed for short-alkyl-chain complexes (**St-1** and **St-2**), while SmA phase (**Fig. 4b**) was predominant for the long-alkyl-chain complexes (**St-8** and **St-12**). A difference was found for **St-4** complexes, which were nematic when complexed with **B-4** and smectic when complexed with **B-6**. For **B-4•St-4, B-6•St-4 and B-6•St-12** the characteristic texture of smectic E (SmE) phase (**Fig. 4c**) was observed. Since this highly ordered phase is structurally related to the SmA phase but with a retained orthorhombic lattice, it usually occurs between the SmA and the crystalline phase.[53] The phase occurred concurrently with Cr and SmA with ambiguous transition temperatures, for which reason it is omitted in **Fig. 3**. The SmE phase has been reported also for pure stilbazoles, but in a different temperature range[41] which, together with the fact that the stilbazoles used in this work are non-liquid-crystalline, pinpoints that the phase is a property of the supramolecular assemblies. The increase in the stability of mesophases by introduction of fluorine into the azobenzene moiety is in line with previous findings[30,38,54] and is attributed to the increase of the overall dipole moment of the assemblies. An overview on the transition temperatures on heating and cooling is reported in table S1 of the Supporting Information.
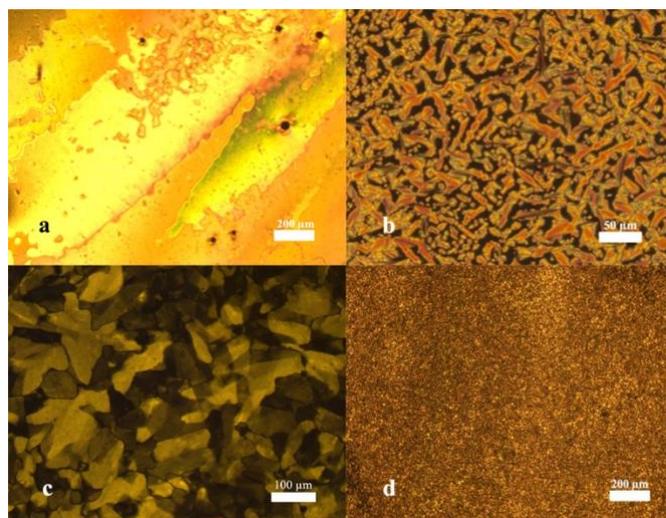


**Fig. 4**. Representative POM images of the relevant phases observed: a) nematic (**B-6•St-1** at 68 °C), b) smectic A (**B-6•St-8** at 111 °C), c) smectic E (**B-6•St-12** at 50 °C), and d) crystalline (**B-6•St-8** at 25 °C).

## Photoinduced phase transitions

In our earlier study[30] we showed that fluorinated iodoazobenzenes halogen bonded to stilbazoles exhibited efficient and reversible photoinduced LC-to-isotropic, and even crystal-to-isotropic, phase transitions due to azobenzene photoisomerization. The mesophases of the difluorinated hydroxyazobenzene complexes studied herein were stable at significantly lower temperatures, which motivated us to compare their photoresponsive phase transition kinetics with our

earlier halogen-bonded complexes. As in our previous study, the complexes were irradiated with 405 nm LED (50 mW/cm$^2$) and observed *in situ* by polarized optical microscopy. As a representative example, the **B-6•St-8** assembly will be discussed in the following; the same behavior was observed for the other complexes as well. The sample was first studied at 90 °C, showing the characteristic focal-conic texture of the smectic A phase (**Fig. 5**). Upon irradiation, the birefringence due to the anisotropic molecular alignment rapidly disappeared, indicating the efficient photo-induced phase transition into the isotropic phase. This phase transition can attributed to the *trans–cis* isomerization of the azobenzene molecules (Fig. 2a), and destabilization of the mesophase due to the bent *cis*-azobenzene moieties.[55] When the illumination was ceased, the birefringent textures appeared instantaneously and were fully recovered within few seconds, reflecting the lifetimes of the azophenols measured in acetonitrile solution. The experiment was repeated at 60 °C and 30 °C with similar results. Thus, while the hydrogen-bonded complexes show more stable mesophases as compared to their halogen-bonded counterparts, their response is invariably "dynamic" and relaxes back to the initial state upon ceasing the irradiation, due to the presence of the phenol moiety in the azobenzene. Therefore, the halogen-bonded azobenzene-stilbazole complexes,[38] due to the long *cis*-lifetimes of the azobenzenes, provide a pathway towards bistable supramolecular LCs (provided that the mesophase ranges can be pushed to lower temperatures), yet the azophenol-stilbazole complexes provide a different pathway, being potentially useful in dynamic photonic applications[6] where efficient isomerization and rapid back relaxation are desired.
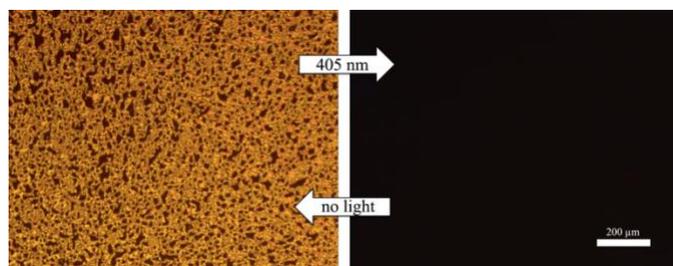


**Fig. 4.** Photoinduced, reversible smectic-to-isotropic phase transition for **St-8•B-6** at 90 °C. Micrographs are taken under POM with crossed polarizers.

## Conclusions

In total, fifteen new hydrogen-bonded photoresponsive supramolecular assemblies were obtained via facile self-assembly process. Comparison between fluorinated and non-fluorinated hydrogen-bond-donating azophenols, complexed to hydrogen-bond-accepting stilbazoles with different alkoxy chain lengths, allowed us to investigate the structure-property relationships of the assemblies and understand the role of *ortho*-fluorination at the azobenzene core for the stabilization of the mesophases. It was shown that difluorination of the phenolic ring increases the overall dipole moment and the strength of the hydrogen bond between the promesogenic azophenol and stilbazole molecules, allowing for the formation of LC phases having significantly enhanced stability compared to those obtained using the non-fluorinated azobenzene (extending over a temperature range > 50 °C upon heating and > 80 °C upon cooling). The complexes also displayed fast and reversible photoinduced phase transitions. We foresee the fluorinated azophenol-based complexes to be of use in dynamic photonic applications. Future work also includes the study of polymeric liquid-crystalline self-assemblies of stilbazoles and fluorinated azophenols.

## Conflicts of interest

There are no conflicts of interest to declare.

## Acknowledgements

## Notes and references

1    T. Kato, M. Yoshio, T. Ichikawa, B. Soberats, H. Ohno and M. Funahashi, *Nat. Rev. Mater.*, 2017, **2**, 17001.

2    J. W. Goodby, I. M. Saez, S. J. Cowling, V. G??rtz, M. Draper, A. W. Hall, S. Sia, G. Cosquer, S. E. Lee and E. P. Raynes, *Angew. Chemie - Int. Ed.*, 2008, **47**, 2754–2787.

3    J. P. F. Lagerwall and G. Scalia, *Curr. Appl. Phys.*, 2012, **12**, 1387–1412.

4    M. Bremer, P. Kirsch, M. Klasen-Memmer and K. Tarumi, *Angew. Chemie Int. Ed.*, 2013, **52**, 8880–8896.

5    C. Tschierske, *Angew. Chem. Int. Ed.*, 2014, **30**, 13499–13509.

6    L. De Sio, N. Tabiryan, T. Bunning, B. R. Kimball and C. Umeton, in *Progress in Optics*, ed. E. B. T.-P. in O. Wolf, Elsevier, 2013, vol. 58, pp. 1–64.

7    Z. Zheng, Y. Li, H. K. Bisoyi, L. Wang, T. J. Bunning and Q. Li, *Nature*, 2016, **531**, 352.

8    X. Chen, L. Wang, C. Li, J. Xiao, H. Ding, X. Liu, X. Zhang, W. He and H. Yang, *Chem. Commun.*, 2013, **49**, 10097–10099.

9    T. J. White, R. L. Bricker, L. V Natarajan, N. V Tabiryan, L. Green, Q. Li and T. J. Bunning, *Adv. Funct. Mater.*, 2009, **19**, 3484–3488.

10    T. J. White, *Photomechanical Materials, Composites, and Systems: Wireless Transduction of Light into Work*, Wiley, 2017.

11    H. M. D. Bandara and S. C. Burdette, *Chem. Soc. Rev.*, 2012, **41**, 1809–1825.

12    T. Ikeda and O. Tsutsumi, *Science (80-. ).*, 1995, **268**, 1873–1875.

13    U. A. Hrozhyk, S. V Serak, N. V Tabiryan, L. Hoke, D. M. Steeves and B. R. Kimball, *Opt. Express*, 2010, **18**, 8697–

8704.

14    D. W. Bruce, *Soft Matter*, 2012, 3493–3514.

15    B. M. Rosen, C. J. Wilson, D. A. Wilson, M. Peterca, M. R. Imam and V. Percec, *Chem. Rev.*, 2009, **109**, 6275–6540.

16    C. Tschierske, *Angew. Chemie Int. Ed.*, 2013, **52**, 8828–8878.

17    C. M. Paleos and D. Tsiourvas, *Liq. Cryst.*, 2001, **28**, 1127–1161.

18    K. Willis, J. E. Luckhurst, D. J. Price, J. M. J. Fréchet, H. Kihara, T. Kato, G. Ungar and D. W. Bruce, *Liq. Cryst.*, 1996, **21**, 585–587.

19    T. Kato and J. M. J. Frechet, *J. Am. Chem. Soc.*, 1989, **111**, 8533–8534.

20    T. Kato, H. Adachi, A. Fujishima and J. M. Frechet, *Chem. Lett.*, 1992, 265–268.

21    T. Kato, H. Kihara, U. Kumar, T. Uryu and J. M. J. Fréchet, *Angew. Chemie Int. Ed. English*, 1994, **33**, 1644–1645.

22    T. Kato, *Science (80-. ).*, 2002, **295**, 2414 LP-2418.

23    T. Kato and J. M. J. Frechet, *Macromolecules*, 1989, **22**, 3818–3819.

24    D. J. Price, K. Willis, T. Richardson, G. Ungar and D. W. Bruce, *J. Mater. Chem.*, 1997, **7**, 883–891.

25    D. W. Bruce and D. J. Price, *Adv. Mater. Opt. Electron.*, 1994, **4**, 273–276.

26    J. Guo, Y. Shi, X. Han, O. Jin, J. Wei and H. Yang, *J. Mater. Chem. C*, 2013, **1**, 947–957.

27    W. He, G. Pan, Z. Yang, D. Zhao, G. Niu, W. Huang, X. Yuan, J. Guo, H. Cao and H. Yang, *Adv. Mater.*, 2009, **21**, 2050–2053.

28    H. Wang, H. K. Bisoyi, L. Wang, A. M. Urbas, T. J. Bunning and Q. Li, *Angew. Chemie Int. Ed.*, 2018, **57**, 1627–1631.

29    Y. Chen, H. Yu, L. Zhang, H. Yang and Y. Lu, *Chem. Commun.*, 2014, **50**, 9647–9649.

30    F. Fernandez-Palacio, M. Poutanen, M. Saccone, A. Siiskonen, G. Terraneo, G. Resnati, O. Ikkala, P. Metrangolo and A. Priimagi, *Chem. Mater.*, 2016, **28**, 8314–8321.

31    G. W. Gray, K. J. Harrison and J. A. Nash, *Electron. Lett.*, 1973, **9**, 130–131.

32    P. Kirsch and M. Bremer, *Angew. Chem. Int. Ed.*, 2000, **39**, 4216–4235.

33    M. Hird, *Chem. Soc. Rev.*, 2007, **36**, 2070–2095.

34    D. O'Hagan, *Chem. Soc. Rev.*, 2008, **37**, 308–319.

35    C. Tschierske, ed. C. Tschierske, Springer Berlin Heidelberg, Berlin, Heidelberg, 2012, pp. 1–108.

36    M. Pfletscher, C. Wölper, J. S. Gutmann, M. Mezger and M. Giese, *Chem. Commun.*, 2016, **52**, 8549–8552.

37    M. Pfletscher, S. Hölscher, C. Wölper, M. Mezger and M. Giese, *Chem. Mater.*, 2017, **29**, 8462–8471.

38    M. Spengler, R. Y. Dong, C. A. Michal, M. Pfletscher and M. Giese, *J. Mater. Chem. C*, 2017, **5**, 2235–2239.

39    M. Giese, T. Krappitz, R. Y. Dong, C. A. Michal, W. Y. Hamad, B. O. Patrick and M. J. MacLachlan, *J. Mater. Chem. C*, 2015, **3**, 1537–1545.

40    M. Spengler, R. Y. Dong, C. A. Michal, W. Y. Hamad, M. J. MacLachlan and M. Giese, *Adv. Funct. Mater.*, 2018, 1800207.

41    D. W. Bruce, D. A. Dunmur, E. Lalinde, P. M. Maitlis and P.

Styring, *Liq. Cryst.*, 1988, **3**, 385–395.

42    J. Garcia-Amoros and D. Velasco, *Phys. Chem. Chem. Phys.*, 2014, **16**, 3108–3114.

43    J. Garcia-Amorós, A. Piñol, H. Finkelmann and D. Velasco, *Org. Lett.*, 2011, **13**, 2282–2285.

44    M. Poutanen, Z. Ahmed, L. Rautkari, O. Ikkala and A. Priimagi, *ACS Macro Lett.*, 2018, **7**, 381–386.

45    P. Hiekkataipale, T. I. Löbling, M. Poutanen, A. Priimagi, V. Abetz, O. Ikkala and A. H. Gröschel, *Polymer (Guildf).*, 2016, **107**, 456–465.

46    D. Bléger, J. Schwarz, A. M. Brouwer and S. Hecht, *J. Am. Chem. Soc.*, 2012, **134**, 20597–20600.

47    C. Knie, M. Utecht, F. Zhao, H. Kulla, S. Kovalenko, A. M. Brouwer, P. Saalfrank, S. Hecht and D. Bléger, *Chem. - A Eur. J.*, 2014, **20**, 16492–16501.

48    J. Garcia-Amoros, A. Sanchez-Ferrer, W. A. Massad, S. Nonell and D. Velasco, *Phys. Chem. Chem. Phys.*, 2010, **12**, 13238–13242.

49    J. García-Amorós and D. Velasco, *Beilstein J. Org. Chem.*, 2012, **8**, 1003.

50    V. Percec, M. Glodde, G. Johansson, V. S. K. Balagurusamy and P. A. Heiney, *Angew. Chemie Int. Ed.*, 2003, **42**, 4338–4342.

51    X. Li, B. Jin, Y. Gao, D. W. Hayward, M. A. Winnik, Y. Luo and I. Manners, *Angew. Chemie Int. Ed.*, 2016, **55**, 11392–11396.

52    F. Liu, R. Kieffer, X. Zeng, K. Pelz, M. Prehm, G. Ungar and C. Tschierske, *Nat. Commun.*, 2012, **3**, 1104–1107.

53    J. Demus, J. W. Goodby, G. W. Gray, H. W. Spiess and V. Vill, *Handbook of Liquid Crystals, Vol. 1*, Wiley-VCH, Weinheim, Germany, 1998.

54    J. P. W. Wong, A. C. Whitwood and D. W. Bruce, *Chem. - A Eur. J.*, 2012, **18**, 16073–16089.

55    T. Ikeda, *J. Mater. Chem.*, 2003, **13**, 2037–2057.